Advances in Wind Engineering 1 (2024) 100011

Contents lists available at ScienceDirect

Advances in Wind Engineering

journal homepage: www.keaipublishing.com/en/journals/awe

Post-disaster investigations of damage feature of buildings and structures due to several local strong winds in China during 2021–2024

Qingshan Yang[a,b,*], Jiaqi Yin[a], Min Liu[a,b], Yu Wang[a], Yi Hui[a,b], Shuangxian Li[a], Guanzhong Wang[a], Youjia Zuo[a], Weicheng Hu[c], Nufeng Nie[a], Jiaxing Wang[a], Kunpeng Cui[d], Lin Da[a], Bowen Jiang[e], Yang Lei[a], Haile Li[a], Xiao Li[a,b], Quanzhou Liu[a], Yingzhu Meng[a], Dahai Wang[f], Jingxue Wang[g], Ze Wang[a], Saeed Hamza[a]

[a] School of Civil Engineering, Chongqing University, Chongqing 400044, China
[b] Chongqing's Key Laboratory of Structural Wind Engineering and Wind Resource Utilization, Chongqing 400044, China
[c] School of Transportation Engineering, East China Jiaotong University, Nanchang 330013, China
[d] China Fire and Rescue Institute, Beijing 102202, China
[e] Research and Development Center, Dongfang Electric Machinery Co. Ltd., Deyang 618000, China
[f] Department of Civil Engineering, Wuhan University of Technology, Wuhan, Hubei 430070, China
[g] School of Soil and Water Conservation, Beijing Forestry University, Beijing 100083, China

ARTICLE INFO

Keywords:
Tornadoes
Downbursts
Poster-disaster investigation
Structural damage features
Numerical simulation

ABSTRACT

Local strong winds such as tornadoes and downbursts are rare in terms of measured wind speed data due to their rapid formation and strong destructive power. Post-disaster investigations have become an important approach for rating the strength of these two kind of winds and analyzing structural failure mechanism. From 2021 to 2024, several tornadoes and downbursts occurred in China. This study delineated changes in the intensity levels of wind disasters along their paths based on on-site disaster investigations and established standards for the level of structural damage based on the extent of functional loss and repair. This study focused on the damage feature to light steel structures, masonry structures, steel-concrete structures, and pole structures, and discussed the causes of the damage from the perspectives of construction and force transmission mechanisms. In addition, this study estimated the equivalent wind speeds based on the damage feature of pole structures and metal roof claddings. To reproduce the damage process for a group of high-rise buildings, the computational fluid dynamic (CFD) technology is used to simulate the airflow distribution inside buildings under two conditions of open and closed interior doors. The investigation results can provide useful information for the wind intensity classification and rating standards in China. Meanwhile, compared with the interior doors being open or closed, closing indoor doors during strong winds can significantly reduce indoor wind speeds, which is beneficial for ensuring safety.

1. Introduction

During the period from 2021 to 2024, China witnessed several extreme wind disasters, leading to severe losses of life and property. The tornado and downburst were two common types of strong winds. Both downbursts and tornadoes are locally destructive strong winds that are difficult to capture due to the sparse distribution of meteorological observation stations. Therefore, post-disaster damage investigation becomes a main way to analyze the intensity of wind disasters.

Tornado is a sudden and highly destructive small-scale atmospheric vortex phenomenon that occurs in severe convective weather conditions, making its prediction difficult. The intensity of tornadoes is usually assessed based on the on-site disaster situation. Fujita (1971) first proposed the strength grading standard of tornadoes, which was later referred to as the Fujita scale (F Scale), aimed at determining the equivalent wind speed and strength level of tornadoes based on the extent of damage to on-site disaster indicators (such as trees, power poles, chimneys, houses, cars, etc.), and later improved to the enhanced

Peer review under the responsibility of the Editorial Board of *Advances in Wind Engineering*.
* Corresponding author.
E-mail address: qshyang@cqu.edu.cn (Q.S. Yang).

https://doi.org/10.1016/j.awe.2024.100011
Received 19 August 2024; Received in revised form 5 October 2024; Accepted 6 October 2024
Available online 10 October 2024
2950-6018/© 2025 The Authors. Publishing services by Elsevier B.V. on behalf of KeAi Communications Co. Ltd. This is an open access article under the CC BY-NC-ND license (http://creativecommons.org/licenses/by-nc-nd/4.0/).

Fujita scale (EF Scale) based on engineering actual conditions (McDonald and Mehta, 2006). Currently, tornado rating standards in various countries are based on the EF Scale, which is modified through the localization of disaster indicators, types of destruction, and corresponding wind speeds. China's damager investigation started relatively late, generally beginning in the 1970s, there is a lack of relevant tornado-related data in China compared to the relatively abundant data accumulation for typhoon wind disaster research (Song and Ou, 2010; Jin et al., 2010; Huo et al., 2016). In recent years, the frequency of tornado occurrences and disaster losses have been increasing, leading to more poster-disaster damage investigations. These investigations can mainly include two parts according to their key concerns: (i) the investigations focusing on meteorology, (ii) the investigations focusing on engineering structure. The first part mainly pays particular attention to the causes, time, location, and path of tornadoes (Chen et al., 1999; Tang and Liao, 2007; Feng et al., 2009; Yamane et al., 2010a, 2010b). The second part focus on the damage level, damage feature and mechanism of engineering structures (Meng and Yao, 2014; Zheng et al., 2016a; Gao, 2018; Yang et al., 2018; Huang et al., 2021; Qiao et al., 2022; Wang et al., 2022). The GB/T 34301-2017 (SAC/TC 345, 2017) issued by China directly uses the EF Scale in order to determine the damage level of tornadoes, which requires the further validation of applicability to the engineering structures in China. From the above literatures, it can be seen that the causes, time, location, and path of tornadoes is basically clear. However, there is a noticeable lack of analysis of strong damage to civil and industrial buildings under tornadoes, and there is an urgent need for the accumulation of relevant work to provide more support for structural wind-resistant research in China. In addition, it is also lacking in current research that the identification of disaster indicated structure and the level of damage based on the damage feature after tornadoes in China (Yang et al., 2023).

Downburst is another local strong wind characterized by a short and strong sudden downward air stream and a near-surface radial burst of strong wind. There is no clear basis for grading the intensity of a downburst, generally assessed based on the scale of tornado intensity combined with on-site disaster situations. In history, downburst occurrences have caused serious harm to the economy, society, and even public life and property safety. However, there are fewer post-disaster damage investigation of downburst disasters, and even fewer criteria for classifying downburst disaster scale specifically, which have to be subordinated to the EF Scale for tornadoes. Established studies have focused on the effects of downburst disasters on (i) airliner (Ding, 2010; Zhao and Yang, 2009), (ii) passenger ship (Zheng et al., 2016b), (iii) transmission line (Xie et al., 2006) and alone training venue (Trautner et al., 2013). Compared to tornado disaster research, current poster-disaster damage investigation of downburst lack a systematic study of the entire disaster area, with more insufficient analysis of the wind-induced damage of structures by downbursts. Meanwhile, the damage ratings for downburst should also be proposed based on the damage feature of engineering structures.

In this article, several tornadoes and downbursts, occurred in China during 2021–2024, are poster-disaster investigated through on-site field investigations. The basic information is provided such as the path, duration, and intensity variations of tornadoes and downbursts. Classification standards are proposed for structural damage ratings, and damage ratings are determined along the path and for structure, along with the statistical analysis of the features and causes of various structural damages. This provides an important scientific basis for determining the failure mechanisms of structures under the two types of wind disasters and optimizing the structural design of wind-prone areas.

2. Past local strong wind hazards in China during 2021–2024

From 2021 to 2024, the research team conducted comprehensive investigations of some destructive wind events, including tornadoes and downbursts, occurred in China. The basic information and damage features were acquired by combining drone aerial surveys with detailed on-site photography. The aforementioned wind events are divided into two kinds, namely tornadoes and downbursts, and introduced separately as follows.

2.1. Overview of several tornadoes

This section primarily presents an overview of investigated tornado disasters.

2.1.1. Wuhan, Hubei Province

At 20:39 on May 14, 2021, Wuhan's Caidian District experienced a sudden severe convective weather event, with the wind exceeding level 9. Due to the lack of scene photos and videos, the kind of this strong wind event was only decided by post-disaster investigation, which indicated that the strong wind disaster exhibited tornado features with large aspect ratio and convergence damage. The intensity level of this event was determined to be EF3 based on the EF Scale (Li et al., 2022). The damage path was from west to east, with a length of approximately 18 km. Based on the collected information, only the severe regions from Xinji Village to Qianzishan Circular Economy Industrial Park were investigated, as shown in Fig. 1.

Under the influence of this tornado, many masonry structures collapsed, large factory sheds were damaged, and a substantial number of trees were broken by the strong winds. Fig. 2 shows wind damage to factory roofs.

2.1.2. Shangzhi City, Heilongjiang Province

At around 17:30 on June 1, 2021, a tornado occurred in Shangzhi City, Heilongjiang Province. Fig. 3 shows a photograph taken on-site of the tornado. According to report, this tornado successively attacked four towns: Mao'ershan, Wujimi, Hedong, and Changshou, resulting in the severe destruction of houses and some injuries. The post-disaster situation is shown in Fig. 4.

By investigating the damage to nearby buildings, it was found that the path of the wind disaster moved from southwest to northeast, as illustrated in Fig. 5, with an average moving speed of 12.7 m/s. Based on the EF Scale, the intensity of tornado in Shangzhi was determined to be EF3 (Xu et al., 2022).

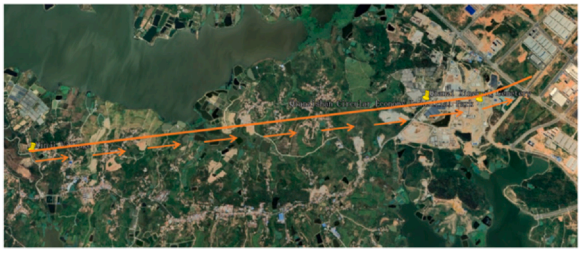

Fig. 1. Damage path of Wuhan tornado.



Fig. 2. Damage to factory buildings.



Fig. 3. Shangzhi tornado.



Fig. 4. Damage to houses.

2.1.3. Shen County, Shandong Province

At 18:00 on July 11, 2021, a tornado struck Shen County, Shandong Province, and caused plenty of damage to trees, electric poles, cars and roofs of light steel factories. The post-disaster situation is shown in Fig. 6. The tornado moved from south to north, as shown in Fig. 7, with a total path length of approximately 19.5 km. Based on the assessment by meteorological experts and on-site investigations, the intensity of this tornado in Shen County was classified as EF2 (Zhi et al., 2022).

2.1.4. Foshan, Guangdong Province

At approximately 7:20 a.m. on June 19, 2022, a tornado occurred in Foshan City, Guangdong Province. The nearest meteorological station in Yayao Primary School (about 200 m away from the center of damage path) recorded a maximum 3-s gust wind speed of 10.5 m/s (level 5). This low wind speed may be due to the small scale of the tornado and its approaching end of life. The tornado damage path was identified by the on-site investigations, as shown in Fig. 8, with a total length of approximately 2.7 km. The Foshan Meteorological Bureau classified the tornado intensity as EF1 (Huang et al., 2023). There were a large



Fig. 6. Post-disaster damage situation.

number of trees, billboards and roof panels blown down by strong winds. Fig. 9 shows wind-induced damage to roof panels.

2.1.5. Guangzhou, Guangdong Province

From 13:00 to 19:00 on April 27, 2024, Guangzhou experienced severe convective weather accompanied by heavy rainfall. A strong tornado occurred in Baiyun District, affecting Guangming Village, Chendong Village, Jinpen Village, and Liangtian Village in Zhongluotan Town. On-site investigations determined the affected areas and the tornado path, as shown in Fig. 10.

During the tornado's movement, the maximum gust wind speed recorded at Maofeng Mountain in Taihe Town, Baiyun District, was 40.4 m/s (level 13). The meteorological station in Liangtian Village, approximately 2.8 km from the tornado's origin, recorded a maximum gust wind speed of 20.6 m/s (level 8). Yang et al. (2023) defined the damage rating of

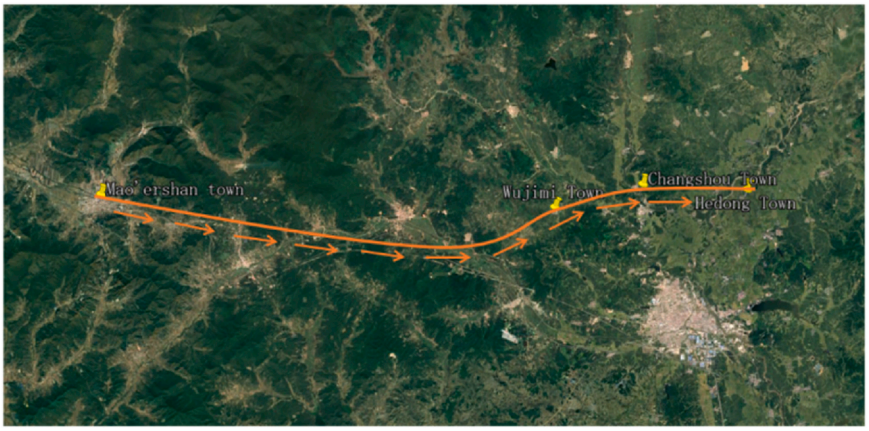

Fig. 5. Damage path of Shangzhi tornado.



Fig. 7. Damage path of Shen County tornado.



Fig. 8. Damage path of Foshan tornado.



Fig. 9. Damage to building roof panels.

different building structures as three types: (i) minor damage, (ii) moderate damage and (iii) severe damage. The damage severity along with Guangzhou tornado path was derived as shown in Fig. 10.

According to local authorities, the disaster resulted in 5 deaths and 33 injuries, with multiple factories and residential buildings damaged. The wind disaster situation is shown in Fig. 11. The Guangdong Meteorological Department assessed the tornado's intensity as strong, classifying it as an EF2 (McDonald and Mehta, 2006).

2.2. Overview of a downburst in Nanchang, Jiangxi Province

Section 2.1 provided an overview of tornado disasters. This section primarily introduces the disaster situation of a downburst investigated during the survey. In the early hours of March 31, 2024, parts of Nanchang City, Jiangxi Province experienced sudden, short-duration heavy rainfall, thunderstorm gusts, and other severe convective weather conditions, which showed the characteristics of downburst. The downburst in Nanchang was determined to be an EF1 based on the EF Scales for tornado classification (McDonald and Mehta, 2006).

Through on-site investigations, Fig. 12 depicts the main affected areas of this wind disaster, where numerous buildings suffered wind damage. Fig. 13 shows a factory near Nanchang Avenue, demonstrating extensive damage caused by the strong winds at the windward edge.

Therefore, the intensity of several tornadoes and a downburst in China during 2021–2024, based on the above analysis, can be obtained combined with the EF Scales. The wind disaster levels of the 5 tornado events investigated by the research team are EF1–3, and the wind disaster level of the downburst is EF1.

3. Wind damage features of various buildings and structures

This section analyzes the damage characteristics of various types of structures, including light steel structures, masonry structures, reinforced concrete buildings, and vertical pole structures. Also, the causes of structure failure are discussed from the aspects of structural configuration and force transmission mechanism.

3.1. Light steel structures

The investigations revealed that light steel structures, mainly used in industrial workshops and temporary buildings, are heavily affected by strong wind events. Light steel structures are more susceptible to wind loads due to the weight. Additionally, the roof panels and purlins are mostly simply lapped and fastened with screws, resulting in poor wind resistance. Therefore, these structures always suffer different degrees of wind-induced damage during local wind hazards.

Fig. 14 shows a light steel factory building in the Yayao Industrial Zone affected by the tornado in Foshan in 2022 (described in Section 2.1.4). It can be observed that a large number of roof panels were blown off, and some roof trusses and purlins were damaged. Parts of the main frame structures were deformed or collapsed.

Figs. 15 and 16 respectively depict light steel factory buildings of a food company and another factory in Shandong, affected by the tornado in 2021 (described in Section 2.1.3). Aerial drone footage reveals that both buildings experienced roof panels being blown off, steel frames shifting and tilting, and partial collapse of the main building structure. Similar phenomena were observed in the Qianzishan Circular Economy Industrial Park during the Wuhan tornado event in 2021 (described in Section 2.1.1).

Based on the degree of damage to Components & Cladding and the main frame structure, this section classifies the wind-induced damage forms of light steel structures into three distinct stages: minor slight damage, moderate damage, and severe damage. The slight damage

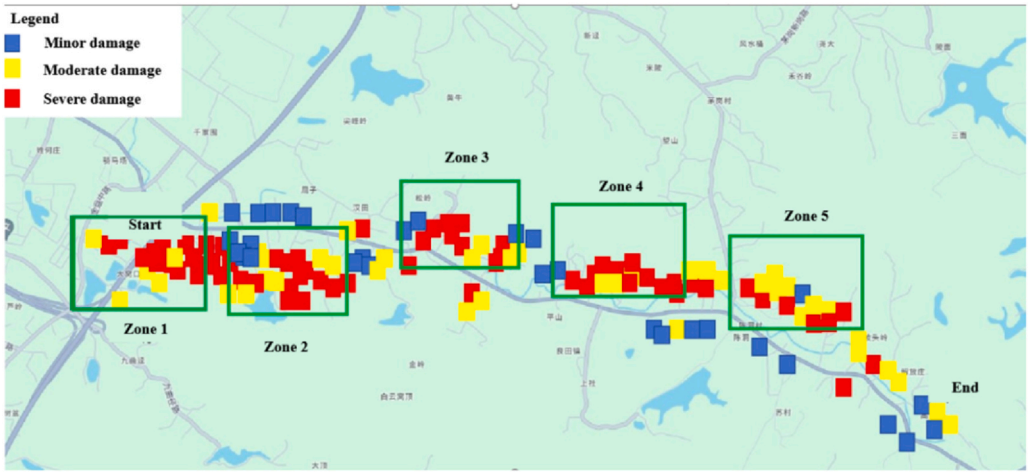

Fig. 10. Guangzhou tornado path and damage severity map.



Fig. 11. Post-disaster damage situation.



Fig. 12. Affected areas.

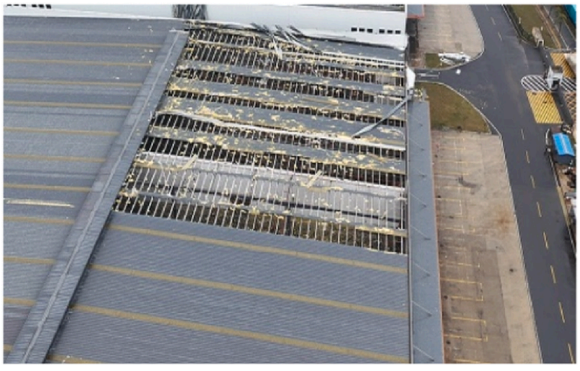

Fig. 13. Damage to factory buildings.

stage means that there is only damage to the Components & Cladding while the main structure remains intact. In this stage, connections between the roof panels and purlins always failed and resulted in extensive roof destruction. Moreover, wind-borne debris further aggravate the roof damage. The moderate damage stage is characterized by damage to both Components & Cladding and main components. Partial rigid-frames often tilted or even collapsed in this stage. The severe damage stage is identified by the collapse of the main structure.

3.2. *Masonry structures*

According to the investigation results, a large number of masonry structures in villages and towns were also major victims in these wind disaster events. Masonry buildings generally use brick walls as vertical load-bearing components, supporting wooden purlins with a covering layer of straw, tiles, or color steel plates. It was found that the purlins are directly supported on triangular endwalls without additional end trusses. Although this method saves materials and allows flexible purlin placement, the lack of effective rigid connection between the roofing structure and the walls results in poor overall integrity and wind resistance. Additionally, the design and construction of these houses did not follow national standards and have deteriorated over time, making them highly susceptible to severe damage in strong wind events.

Figs. 17 and 18 respectively show the damage observed in masonry structures during the tornado event in Shangzhi, Heilongjiang in 2021(described in Section 2.1.2). Fig. 17 reveals that these houses always suffer roof panel damage such as tiles being blown off and entire roof structures being lifted off, accompanied by door and window damage due to flying debris. Fig. 18 shows that under stronger wind forces, the roof structure of masonry buildings may be destroyed heavily, even leading to the collapse of the main structural walls.



Fig. 14. The components and cladding of light steel structure were damaged.

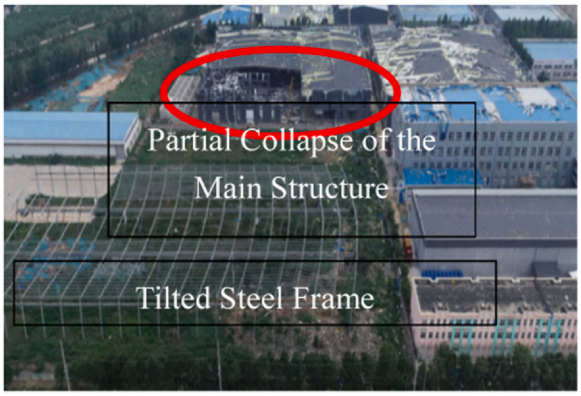

Fig. 15. The light steel structure roof was lifted off, part of the main factory building structure collapsed, and the steel frame tilted.



Fig. 16. The main frame structure of the light steel structure was deformed and collapsed.

In the 2024 downburst event in Nanchang, Jiangxi Province (described in Section 2.2), similar damage characteristics of masonry structures were observed, as shown in Fig. 19.

The damage characteristics of masonry structures under strong wind consist of three main aspects by analyzing the investigation results: tiles and roof panels being blown off, roof damage, and collapse of the main frame structure. In such strong wind events, the roof has to rely solely on its own weight to resist the wind. If there is a lack of effective constraint between the roof and the walls, the roof is prone to being blown off. Given that tornadoes are accompanied by significant pressure drops, which generate higher vertical lift than ordinary horizontal winds, the coupling suction on the roof structure is increased, making it more susceptible to being lifted. Once the roof structure is blown off, the surrounding walls, missing the out-of-plane constraints, experience a significant stiffness decrease in out-of-plane direction and are more likely to collapse under the effects of tornadoes.

3.3. *Reinforced concrete buildings*

Compared with light steel structures and masonry structures, good integrity and high stiffness are the main advantages of reinforced concrete buildings for wind resistance. According to the investigation results, the primary damage occurred in reinforced concrete buildings include broken exterior walls, doors and windows, and roof materials being blown off.

Fig. 20 shows the damage to teaching buildings at Shenzhou Middle School in Shen County tornado (described in Section 2.1.3). It is shown that there was severe damage to the building's external walls and windows.

Figs. 21 and 22 show the investigated phenomena of two residential areas in Shen County. Fig. 21 show the wind-induced damage in residential community A, where roof tiles were blown off, windward window frames fell off entirely, and wall panels in the leeward elevator shaft detached.

Similarly, Fig. 22 shows the wind-induced damage in residential community B, including large-scale loss of roof tiles and decorative items, damage to exterior walls, and broken doors and windows.

In the 2024 Nanchang downburst event, as shown in Fig. 23, both high-rise buildings and lower residential houses in a certain community exhibited similar damage characteristics.

Overall, the damage to reinforced concrete buildings during strong wind events mainly occurs in Components & Cladding, with the main damage characteristics being the loss of decorative roof tiles, damage to exterior wall materials, and the destruction of doors and windows. Once the roof materials are blown off, they become high-speed flying debris, impacting the exterior walls and causing damage and functional impairment to the building.

3.4. *Vertical pole structures*

During the investigation, the research team found that in addition to light steel structures, masonry structures, and reinforced concrete structures, vertical pole structures such as signs, utility poles, and streetlights also exhibited common damage characteristics in wind disaster events. Fig. 24 shows the deformation and collapse of a photovoltaic streetlight pole at its base due to strong winds, observed outside a residential area during the 2024 downburst event in



(a) Roof tiles of masonry structures in Guangming Village were lifted off

(b) Roof and windows damage of masonry structure houses in Guangming Village

Fig. 17. Disaster situation in Guangming Village during the Harbin Shuangcheng tornado event in Heilongjiang Province.



(a) Damaged roof of masonry structure houses in Changxin Village.

(b) Collapsed Walls of masonry structure houses in Changxin Village

Fig. 18. Disaster situation in Changxin Village during the Harbin Shuangcheng tornado event in Heilongjiang Province.



(a) Roof tiles of houses in a certain village in Nanchang were lifted off and the roof was damaged

(b) Roof of a house in a certain village in Nanchang was damaged, and the main structure collapsed

Fig. 19. Disaster situation in a certain village during the Nanchang downburst event.

Nanchang (described in Section 2.2). Similarly, another streetlight outside a logistics park experienced base failure and severe bending deformation of its main structure.

In summary, the main damage forms of vertical pole structures can be categorized into three types, which are the shifted and inclined structure, yield deformation at the base of the structure and tear damage at the base of the structure.

This section has systematically analyzed the damage characteristics of wind-induced disasters from four structural perspectives: light steel structures, masonry structures, reinforced concrete structures, and vertical pole structures. It's worth noting that differences in intensities of strong wind events and building positions relative to damage path were the two main reasons why buildings with similar wind resistance suffered various degrees of damage. Moreover, the center of damage path is a relatively more dangerous position for buildings due to the coupling effect of pressure drop and wind speed. Based on the aforementioned investigation results and the tornado damage classification table proposed by Yang et al. (2023), a new classification table, including more damage indicators, for the classification of wind-induced -damage has been established, as shown in Table 1.

According to the investigation and analysis in Section 3, light steel structures such as metal roof claddings may suffer the one of the most



(a) Exterior wall damage (b) Severe window damage

Fig. 20. Shen County Middle School building damage in Shen County tornado.

severe wind damage. The most common cause of failure of metal roof claddings is damage to the metal panels at the pierced fixed or seam-clip connections. Therefore, it is critical to correctly assess the wind loads on the roof and the wind resistance capacity at the pierced fixed or seam-clip connections and to take reasonable wind-resistant reinforcement measures in the wind-resistance design code. Meanwhile, a common type of damage to masonry structures is wind damage to roof tiles, which, because they're resting directly on the roof, are less able to resist wind suction. This type of damage can also result in damage from flying objects, which can have a serious impact on the safety of residents' lives and property, so wind reinforcement measures for roofs of this type of building should be worthy of attention in the wind-resistance design code. Moreover, the damage to reinforced concrete buildings is mainly due to pressure or suction damage to windows and doors. In addition to correctly assessing the wind load and resistance capacity of such structures, consideration should also be given to preventing people from falling from the interior of such buildings after the windows and doors have been damaged, so the rational design of railings is very important.

4. Equivalent wind speed estimation of wind disaster

Local strong winds such as tornadoes and downbursts are rare in terms of measured wind speed data due to their rapid formation and strong destructive power. This results in a lack of precise and effective wind speed data for strong wind events. Estimating the equivalent wind speed during strong wind events is crucial for wind disaster investigations, which can validate the applicability of the code GB/T 34301-2017 (SAC/TC 345, 2017) to the engineering structures in China. This section will present cases of equivalent wind speed estimation for two types of structures based on the investigation results.

4.1. Yield failure of a photovoltaic streetlight pole

The first case is from the investigation of the downburst in Nanchang, Jiangxi Province in 2024, as described in Section 2.2. Photovoltaic streetlight poles around an open area outside a residential community experienced yield deformation at the base due to the impact of the downbursts, as shown in Fig. 25.



(a) Roof tiles lifted off



(b) Window frames detached in the Windward Side



(c) Elevator shaft wall panels detached in the Leeward Side

Fig. 21. Damage situations in residence community A.



(a) Extensive roof tile lift-off



(b) Exterior wall damage

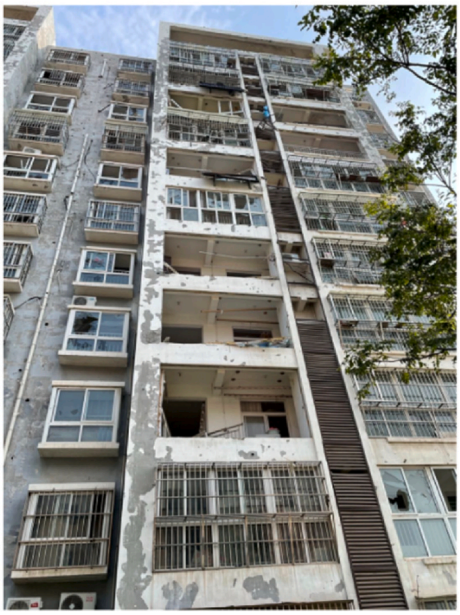

(c) Window damage

Fig. 22. Damage situation in residence community B.

It can be assumed that the structural failure of the pole occurred when the base bending moment exceeded the ultimate moment of resistance based on on-site investigation results.

$$M_w \geq M_p \tag{1}$$

where M_p, M_w are the ultimate moment of resistance and the base bending moment, respectively. And M_w could be determined by Eq. (2).

$$M_w = F_n l_u \tag{2}$$

where the wind load arm $l_u = 5.68$ m based on the on-site measurements. The wind load F_n at the top of the pole can be calculated:

$$F_n = \frac{1}{2}\rho V_n^2 C_{fig} A_b \tag{3}$$

where $\rho = 1.225$ kg/m^3, V_n, C_{fig}, A_b are the air density, the 3-s gust wind speed at the top of the pole, the aerodynamic shape coefficient, and the vertical projection area of the photovoltaic panel, respectively. According to AS/NZS1170.2 (Australasian Wind Engineering Society, 2022)



(a) High-rise Building Damage in a Nanchang Community



(b) Low-rise House Damage in a Nanchang Community

Fig. 23. Damage situation in a Nanchang community.




Fig. 24. Pole structure damage observed in Nanchang.

Table 1
Classification of wind-induced damage to structures.

Structure Type	Damage Classification		
	Minor Damage	Moderate Damage	Severe Damage
Light Steel Structure	Components and Cladding is damaged but main structure remained intact  Roof panels, doors, and windows damaged	Partial damage to main components  Extensive damage can be observed on the roof	The main structure collapsed  The roof destroyed and main structure collapsed
Masonry Structure	 Part of the roof panels have been blown off	 Extensive damage can be observed on the roof	 The roof destroyed and main structure collapsed
Reinforced Concrete Structure	 The roofing material has been blown off	 The windows, roof, and exterior walls are damaged	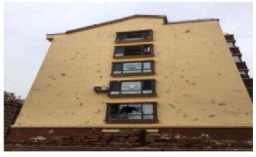 The windows are damaged and the exterior walls are severely destroyed
Vertical Pole Structure	 The structure has shifted and inclined	 Yield deformation at the base of the structure	 Tear damage at the base of the structure



Fig. 25. Yield damage of solar panel lamp post.



Fig. 26. Metal roof cladding damage of university gymnasium.

and on-site measurement data, the aerodynamic shape coefficient $C_{fig} = 1.2$, and the vertical projection area of the photovoltaic panel $A_b = 0.36\ m^2$. The ultimate moment of resistance M_p in Eq. (1) can be calculated using Eq. (4).

$$M_p = 2f_y s \tag{4}$$

where $f_y = 235\ N/m^2$ is the yield strength of the material, and the section modulus s is given by Eq. (5).

$$s = \pi(d_1^4 - d_2^4)/(32d_1) \tag{5}$$

where $d_1 = 0.13$ m, $d_2 = 0.1295$ m are the outer diameter, inner diameter as measured on-site.

The 3-s gust wind speed at the height of the pole can be estimated to be around 32.0 m/s by Eq. (3). Converting this to the 10-m height standard for Class B terrain using an exponential law with $a = 0.15$, the 3-s gust wind speed at 10 m is calculated to be 34.8 m/s. The 3-s gust wind speed for this failure phenomenon corresponds to 44 − 62 m/s by referring to the GB/T 40243-2021 (China Meteorological Administration, 2021).

4.2. Failure of metal roof claddings

The second case also comes from the investigation of the downburst in Nanchang, Jiangxi Province in 2024. According to the investigation results, the metal roof claddings of the gymnasium at a university suffered wind-induced uplift damage, as shown in Fig. 26.

It is known that the wind suction exceeded the wind-resistance capacity of the roof claddings based on the principles of structural reliability, which can be determined by Eq. (6).

$$P_w \geq P_p = 1.5\ \text{kPa} \tag{6}$$

where $P_p = 1.5$ kPa is the wind-resistance capacity of the roof, and P_w is the wind suction, which can be determined by Eq. (7).

$$P_w = \frac{1}{2}\rho V_n^2 \mu_s \tag{7}$$

where $\rho = 1.225\ kg/m^3$, V_n, μ_s are the air density, 3-s gust wind speed at the roof height, and the roof shape coefficient. The roof shape coefficient is determined based on the wind direction inferred from the damage characteristics and in combination with the GB50009-2012 (Housing and Urban-Rural Development of the People's Republic of China, 2012) as 1.10.

For Class B terrain, using the exponential law $a = 0.15$, the 3-s gust wind speed at the roof height can be calculated as around 47.2 m/s. The 3-s gust wind speed corresponding to this damage phenomenon should be within a specific range by referring to the GB/T40243–2021 (China Meteorological Administration, 2021).

It is shown that the estimated wind speeds from equivalent wind speed estimation and the EF Scales matched very well, which means the validity of the code GB/T 34301-2017 (SAC/TC 345,2017) issued by China directly uses the EF Scale. Meanwhile, these damage indicators, like poles and roof claddings, can be applied in the editing Chinese EF Scale for tornadoes and downbursts.

5. Numerical simulation of the damage process

Numerical simulation plays a crucial role in the post-analysis of wind disasters. Through numerical simulation, the occurrence process of wind disasters can be recreated and their impacts assessed. This helps deepen the understanding of the physical mechanisms and disaster characteristics of wind disasters, providing a scientific basis for post-disaster recovery and disaster prevention.

The accidents occurred on the 11th and 20th floors of the Building 3. The southern balcony of the building was crushed and the western balcony was blown. Since the door was open, convection currents were created and three people living in the west bedroom were blown out the west window and fell to their deaths. Using the wind disaster in Nanchang, Jiangxi Province on March 1, 2024 as an example, this paper aims to replicate the actual layout of buildings and investigate the characteristics of wind loads on building surfaces. Furthermore, it delves into the airflow characteristics inside buildings after windows are damaged.

5.1. Analysis of the incoming wind direction impact

Four different wind directions were considered to analyze the impact of incoming wind direction on the pressure difference inside and outside the west-facing balconies and windows after damage occurs to the south-facing balconies and windows: 45°, 60°, 70°, and 90°. The results indicate that the pressure difference on the west-facing windows of Building 3 reaches its maximum at 60°, making it susceptible to wind-induced damage, as shown in Fig. 27.

5.2. Numerical modeling of wind environments around buildings

A numerical simulation model is establish using commercial software ANSYS for the buildings. Combined with the location of the buildings, it can be determined that the direction of the incoming wind was southwest as shown in Fig. 28. The numerical simulation results at

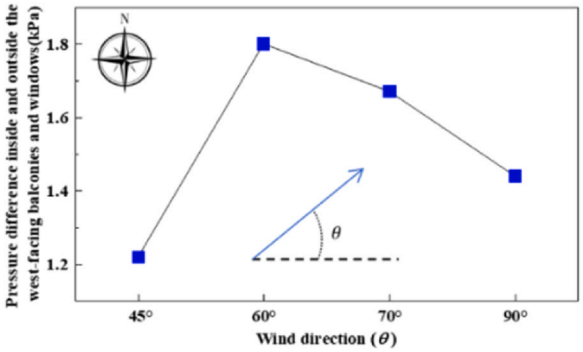

Fig. 27. Analysis of the impact of incoming wind direction.

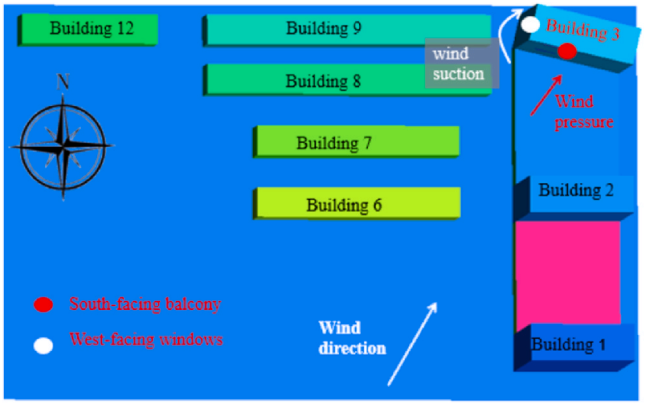

Fig. 28. Schematic diagram of the numerical simulation model.

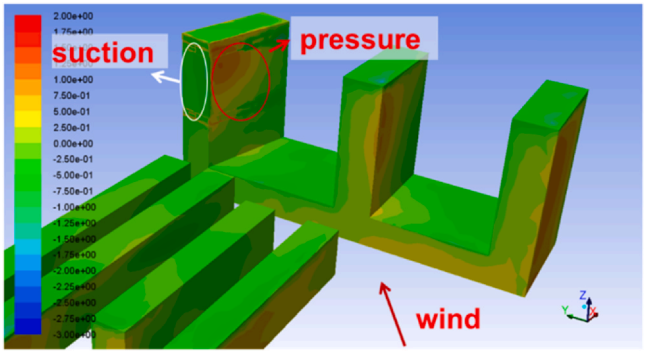

Fig. 29. Numerical simulation results for mean wind pressure coefficient.

60° were mainly analyzed because the west-facing windows of Building 3 reaches its maximum at 60°. The southern balconies of the Building 3 will experience wind pressure under this wind direction, while the western window will experience wind suction due to flow separation and reattachment effects.

In this study, the Reynolds-Averaged Navier-Stokes (RANS) with the SST k-ω model is adopted. The entire computational domain is 12 km (W-E) × 12 km (N-S) × 1.2 km (vertical direction), and the number of grids is about 10 million. In the CFD simulations, the boundary conditions are set as follows: velocity-inlet for the incoming flow, pressure-outlet for the outlet, no-slip wall for the ground, and symmetry for the top boundary and two sides. When the incoming flow is not perpendicular to the inlet surface, the incoming flow is set to flow at a certain angle, and the two outlets will be set as pressure-outlet. The maximum number of iteration steps is set as 3000. Here, convergence criteria for velocity and pressure are chosen as 10^{-6}. Moreover, the velocity of the outlet is monitored to determine whether the flow becomes stable. Reference for details of incoming flow can be found in Hu et al. (2024).

Based on the wind speed at 10 m height of 34.82 m/s and the incoming wind direction from the west-southwest at 60°, which were determined from calculations of damage to photovoltaic panels and lamp posts as well as the direction of windborne projectiles from nearby low-rise house roof tiles, numerical simulations were conducted for the wind environment around the building cluster. The simulation results, as shown in Fig. 29, indicate that the western sides of Buildings 1 and 2 experience both pressure and suction forces. Building 3, positioned at a certain angle relative to Buildings 1 and 2, exacerbates the flow separation and reattachment phenomena on its western side, significantly increasing the effect of wind suction.

Based on the simulation results, the southern balconies of the 20-storey Building 3 experience a wind pressure of 1.90 kPa, while the west-facing windows endure a wind suction of 2.47 kPa. We compared the simulation results of building surfaces subjected to wind pressure and wind suction with the design results. According to the code GB 50009-2012 (Housing and Urban-Rural Development of the People's Republic of China, 2012), design wind loads can be estimated using gust factor β_{gz}, local shape factor μ_{sl}, height variation factor μ_z, and the basic wind pressure w_0 at the building's location.

$$w_k = \beta_{gz}\mu_{sl}\mu_z w_0 \tag{8}$$

Considering the internal and external pressure of the building, the local shape factors for the windward face and the side face of the rectangular cross-section are +1.2 and −1.6, respectively (Housing and Urban-Rural Development of the People's Republic of China, 2012). Here, "+" indicates pressure, and "−" indicates suction.

The gust factor is calculated by the Eq. (9),

$$\beta_{gz} = 1 + 2gI_o\left(\frac{z}{10}\right)^{-\alpha} \tag{9}$$

where g is the peak factor, I_o is the turbulence intensity, z is the height above ground level, and α is the wind profile exponent. The height variation factor for wind pressure is calculated by the Eq. (10):

$$\mu_z = 1.0\left(\frac{z}{10}\right)^{2\alpha} \tag{10}$$

The basic wind pressure at the location of the building can be determined from Appendix in GB 50009-2012 (Housing and Urban-Rural Development of the People's Republic of China, 2012). For Nanchang with a 50-year return period, the basic wind pressure is 0.45 kN/m^2.

The standard values of wind pressure calculated according to GB 50009-2012 (Housing and Urban-Rural Development of the People's Republic of China, 2012) for this high-rise building are a positive pressure value of 1.64 kPa and an extreme negative pressure value of 2.18 kPa. Without considering the partial load factor in the design, these values may potentially be lower than the loads that the building could withstand under such special convective climate conditions.

5.3. Numerical simulation of indoor convection in buildings

When both the windows of the south-facing balcony and the west-facing windows are damaged, and the bedroom door on the west side is left open, the airflow passing through the doorway is rapidly compressed, experiencing the "venturi effect" which causes a sudden increase in wind speed, before flowing out through the west-facing windows, as shown in Fig. 30.

According to the simulation results at the wind direction shown in Fig. 31, the peak 3-s gust wind speed near the west-facing windows exceeds 27 m/s under the influence of the "venturi effect", while the maximum 3-s gust wind speed can reach up to 45 m/s at the doorway passage.

The wind environment of the buildings with both sides of the window destroyed and the inner door closed was simulated in order to analyze the effect of whether the inner door is closed or not on the wind flows. Fig. 32 shows the distribution of wind speed above ground level of the 20th floor when the inner door is closed. It can be noticed that the maximum internal wind speed will decrease from 45 m/s to 8 m/s after closing the

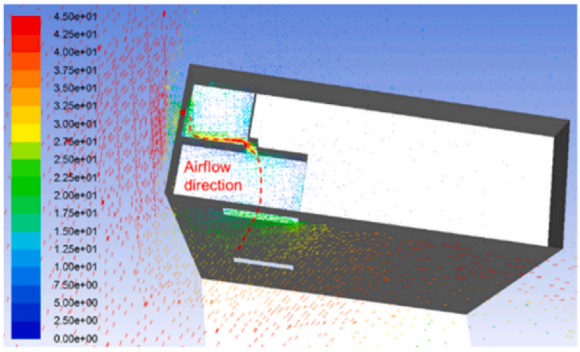

Fig. 30. Numerical simulation of airflow direction (after window damage).

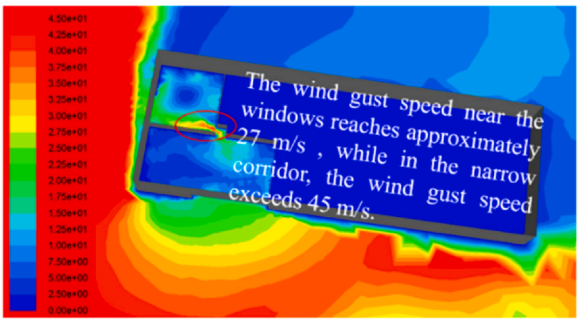

Fig. 31. Numerical simulation result of cross-sectional wind speed (after window damage).

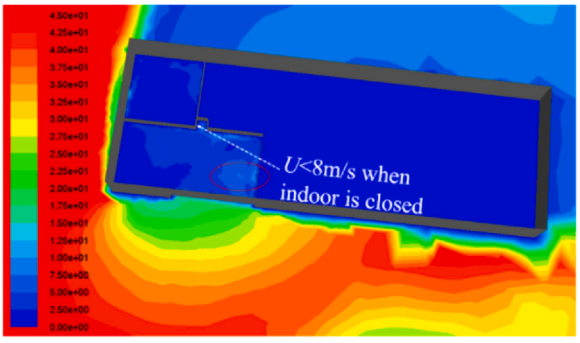

Fig. 32. Numerical simulation results of cross-sectional wind speed (after window damage).

inner door. Apparently, closing inner doors can be very helpful in preventing indoor strong wind damage accidents from occurring.

The numerical simulation process above has revealed the comprehensive impact of factors such as wind speed, wind direction, and building layout on disasters. The simulation results contribute to understanding the underlying mechanisms of wind disasters. Numerical simulation technology provides strong support for research into wind disaster impacts.

6. Conclusion

This article introduces a research overview of multiple tornado and downburst events in China from 2021 to 2024, and the following conclusions have been drawn:

(1) The wind disaster intensity of the 5 tornado events investigated by the research team are EF1-3, and the wind disaster levels of the 1 downburst events are EF1-2 according to the code GB/T 34301-2017 (SAC/TC 345, 2017).
(2) It is concluded that steel-concrete structures have the best wind resistance by researching the damage characteristics of various structures and analyzing the causes, with only cladding and components suffering damage. Light steel structures, due to their light weight and low stiffness, and masonry structures lacking effective connections between roofs and walls, have poor overall integrity. Besides, pole structures, exhibiting bending or snapping damage in the root area, can be regarded as a new damage indicator for classification. Therefore, these structures exhibits varying degrees of damage, and even collapse during the wind disasters, which indicates the requirement of more sufficient wind resistance design. Based on the above structural damage characteristics, this paper gives a damage classification table for different building structures.
(3) Equivalent wind speed estimation is important to realize the damage to buildings during a wind disaster based on the damage indicators. In this paper, the equivalent wind speeds of the two types of structures have been calculated which are mentioned in the EF scale, such as metal building systems (MBS) and light poles. The calculated equivalent wind speeds are very close to the provisions of the EF scale at the time of damage, which proves that the EF scale for the damage level of these two types of structures are applicable to China. These findings align with the conclusions drawn in previous study (Yang et al., 2018). However, considering the lack of construction information and the difference of build quality, the applicability of the remaining 21 types of houses, three types of structures and two types of trees has not been verified and deserves further investigation.
(4) Numerical simulation technology can provide strong support for wind disaster research. It can be concluded from the simulation results that the wind speed of the incoming flow rises from 27 m/s to 45 m/s as it passes through the narrow passageway due to the opening interior door, which is known as "venturi effect". But when the interior door is closed, the wind speed decreases to 8 m/s. Moreover, General residential balconies in order to prevent the catastrophic consequences of the accelerating effect in the interior after such destruction of windows and doors, usually the balcony will have a railing to prevent people and things from being blown down the stairs, the design of this railing is currently immature, the numerical simulation in this paper will be helpful for the reference of the relevant design.

CRediT authorship contribution statement

Qingshan Yang: Writing – review & editing, Supervision, Resources, Project administration, Methodology, Funding acquisition. **Jiaqi Yin:** Writing – original draft, Visualization, Validation, Software, Investigation, Formal analysis, Data curation. **Min Liu:** Writing – review & editing, Supervision, Project administration, Methodology, Conceptualization. **Yu Wang:** Writing – review & editing, Methodology, Data curation. **Yi Hui:** Methodology, Data curation. **Shuangxian Li:** Data curation. **Guanzhong Wang:** Data curation. **Youjia Zuo:** Data curation. **Dahai Wang:** Data curation. **Weicheng Hu:** Writing – review & editing, Data curation. **Jingxue Wang:** Data curation. **Nufeng Nie:** Writing – original draft, Data curation. **Ze Wang:** Data curation. **Jiaxing Wang:** Writing – original draft, Data curation. **Saeed Hamza:** Data curation. **Kunpeng Cui:** Data curation. **Lin Da:** Data curation. **Bowen Jiang:** Data curation. **Yang Lei:** Data curation. **Haile Li:** Data curation. **Xiao Li:** Data curation. **Quanzhou Liu:** Data curation. **Yingzhu Meng:** Data curation.

Declaration of Competing Interest

On behalf of all co-authors, I would like to declare that we have no known competing financial interests or personal relationships that could have appeared to influence the work reported in this paper. Qingshan Yang is an associate editor for *Advances in Wind Engineering* and he was not involved in the editorial review or the decision to publish this article.

Acknowledgments

The authors would like to acknowledge the financial support from National Natural Science Foundation of China (Nos. 52221002, 52178457), Chongqing Science and Technology Talent Training Project (No. CSTB2023YSZX-JCX0007), National Key Research and Development Program of China (No. 2023YFC3008503).

References

Australasian Wind Engineering Society, 2022. Wind Loading Handbook for Australia and New Zealand – Background to AS/NZS1170.2 Wind actions, AWES-HB-001-2022. Australasian Wind Engineering Society.
Chen, J.Y., Yang, H.Y., Zhu, Y.Q., Liu, J.C., Xuan, D.W., Jiang, A.J., Jia, P.R., 1999. Investigation and evaluation of tornado and wind disaster. Journal of Natural Disasters 8, 111–117 (in Chinese).

China Meteorological Administration, 2021. *Grade of tornado intensity: GB/T 40243—2021*. China Standards Press, Beijing (in Chinese).
Ding, L., 2010. Effects of low-level wind shear on flight and its counter-measures. Command Information System and Technology 23, 19–21 (in Chinese).
Feng, Z., Chen, L.S., Zhong, J.F., 2009. Analysis of a strong tornado in the outer-region of the super typhoon "Sepat" in 2007. Proceedings of the WRI World Congress on Computer Science and Information Engineering. 2. IEEE, 283–287.
Fujita, T.T., 1971. Proposed Characterization of Tornadoes and Hurricanes by Area and Intensity (No. NASA-CR-125545). The University of Chicago.
Gao, R., 2018. Tornado Characteristics Statistical Analysis and Post-disaster Investigations in China. Master Thesis. Beijing Jiaotong University, Beijing, China (in Chinese).
The Ministry of Housing and Urban-Rural Development of the People's Republic of China, 2012. Load Code for the Design of Building Structures (GB50009-2012). China Architecture and Building Press, Beijing, China (in Chinese).
Hu, W.C., Yang, Q.S., Yuan, Z.T., Yang, F.C., 2024. Wind farm layout optimization in complex terrain based on CFD and IGA-PSO. Energy 288, 129745.
Huang, S.T., Li, Z.M., Bai, L.Q., Huang, X.X., Zhi, J.L., Xu, Z.H., Liu, Q.J., 2023. Characteristics of tornado activities and disasters in China in 2022. Advances in Meteorological Science and Technology 13, 23–32 (in Chinese).
Huang, X.X., Yu, X.D., Yan, L.J., Cai, K.L., Zhi, J.L., Wang, S.F., 2021. Analysis of the 13 April 2019 Strong Tornado in Xuwen County, Guangdong Province. Meteorological Monthly 47, 216–229 (in Chinese).
Huo, L.S., Wang, Y.K., Li, Y.X., Li, G., Li, H.N., 2016. Investigation of building damage conditions of coastal towns and villages in Fujian province by typhoon "Soudelor". Journal of Disaster Prevention and Mitigation Engineering 2, 315–322.
Jin, Y.F., Yang, Q.S., Li, Q., 2010. Typhoon damage investigation of claddings of light steel buildings. Journal of Building Structures 31, 197-201,231 (in Chinese).
Li, C.L., Yang, B., Yao, D., Fang, C., Peng, S.Q., He, Q.R., Huang, X.X., Cai, K.L., Wu, C.H., Huang, X.Y., He, B., 2022. Damage survey and radar characteristics of the 14th May 2021 Wuhan tornado in Hubei province. Torrential Rain and Disasters 41, 142–150 (in Chinese).
McDonald, J.R., Mehta, K.C., 2006. A Recommendation for an Enhanced Fujita Scale (EF-Scale). Wind Science and Engineering Center, Texas Tech University.
Meng, Z.Y., Yao, D., 2014. Damage survey, radar, and environment analyses on the first-ever documented tornado in Beijing during the heavy rainfall event of 21 July 2012. Weather and Forecasting 29, 702–724.
Qiao, P., Chen, W., Zhao, J., Gao, J.Y., Zhai, G.F., 2022. Factors associated with housing damage caused by an EF4 tornado in rural areas of Funing, China. International Journal of Environmental Research and Public Health 19, 14237.
SAC/TC 345, 2017. Technical Specifications for Tornado Damage Investigation: GB/T 34301-2017. China Standards Press, Beijing (in Chinese).
Song, F.F., Ou, J.P., 2010. Investigation and analysis of structures damage caused by typhoon "Hagubit". Journal of Natural Disasters 19, 9–17 (in Chinese).
Tang, X.X., Liao, Y.F., 2007. An analysis of a tornado in Yongzhou, Hunan Province. Meteorological Monthly 33, 23–28 (in Chinese).
Trautner, C., Ojdrovic, R., Schafer, B.W., Jones, N.P., 2013. An investigation of the collapse of the Dallas Cowboys Practice Facility. Forensic Engineering 2012: Gateway to a Safer Tomorrow. 1268–1277.
Wang, Y.P., Wang, T., Yang, P., Xue, W., 2022. A numerical simulation of the "1907" Kaiyuan tornado weather process in Liaoning, Northeast China. Atmosphere 13, 219.
Xie, Q., Zhang, Y., Li, J., 2006. Investigation on tower collapses of 500 kV Renshang 5237 transmission line caused by downburst. Power System Technology 30, 59–63 (in Chinese).
Xu, Y., Shao, M.R., Tang, K., Zhang, L.B., Du, J., Wang, Y.C., 2022. Multiscale characteristics of two supercell tornados of Heilongjiang in 2021. Journal of Applied Meteorological Science 33, 305–318 (in Chinese).
Yamane, Y., Hayashi, T., Dewan, A.M., Akter, F., 2010a. Severe local convective storms in Bangladesh: Part I. Climatology. Atmospheric Research 95, 400–406.
Yamane, Y., Hayashi, T., Dewan, A.M., Akter, F., 2010b. Severe local convective storms in Bangladesh: Part II: Environmental conditions. Atmospheric Research 95, 407–418.
Yang, Q.S., Gao, R., Bai, F., Li, T., Tamura, Y., 2018. Damage to buildings and structures due to recent devastating wind hazards in East Asia. Natural Hazards 92, 1321–1353.
Yang, Q.S., Wang, Y., Hui, Y., Tian, Y.J., Xie, H., Qian, Z., Wu, H.Q., et al., 2023. Investigation and analysis of structural damage induced by the 3 July tornado in Kaiyuan, Liaoning Province. Journal of Building Structures 44, 183–190 (in Chinese).
Zhao, W.Z., Yang, W.W., 2009. The simulation algorithm design of the safety margin for an aircraft accident. Proceedings of the International Conference on Advanced Computer Control. IEEE, 680–684.
Zheng, Y.G., Zhu, W.J., Yao, D., Meng, Z.Y., Xue, M., Zhao, K., Zheng, Y.Y., 2016a. Wind speed scales and rating of intensity of the 23 June 2016 tornado in Funing County, Jiangsu Province (in Chinese). Meteorological Monthly 42, 1289–1303.
Zheng, Y.G., Zhu, W.J., Yao, D., Meng, Z.Y., Xue, M., Zhao, K., Wu, Z.F., Wang, X.H., Zheng, Y.Y., 2016b. Survey and multi-scale characteristics of wind damage caused by convective storms in the surrounding area of the capsizing accident of cruise ship "Dongfangzhixing" (in Chinese). Meteorological Monthly 42, 1–13.
Zhi, J.L., Huang, X.X., Bai, L.Q., Cai, K.L., Li, C.L., Li, Z.M., Zhang, J.J., Guan, L., Sheng, J., Zhou, K.H., Xu, Z.H., He, Q.R., Mai, W.Q., Peng, S.Q., 2022. Characteristics of tornado activities and disasters in China in 2021. Advances in Meteorological Science and Technology 12, 26–36 (in Chinese).